Electronic Supplementary Material (ESI) for Journal of Materials Chemistry A.

Supplementary Information

Pt-loaded Au@CeO_2 core-shell nanocatalysts for improving methanol oxidation reaction activity

Dung Van Dao,[a,b] Thanh Duc Le,[b] Ganpurev Adilbish,[b] In-Hwan Lee*[c] and Yeon-Tae Yu,*[b]

[a] Institute of Research and Development, Duy Tan University, Danang 550000, Vietnam

[b] Division of Advanced Materials Engineering and Research Center for Advanced Materials Development, Chonbuk National University, Jeonju 54896, South Korea. E-mail: yeontae@jbnu.ac.kr

[c] Department of Materials Science and Engineering, Korea University, Seoul 02841, South Korea. E-mail: ihlee@korea.ac.kr

Additional experimental section

Synthesis of pure CeO_2

Firstly, 1.5 g $Ce(NO_3)_3.6H_2O$ was added to 40 mL of 1 M Na_2CO_3 aqueous solution. The mixture was magnetically stirred for 30 min and transferred into a 50 mL teflon-lined stainless steel autoclave. The autoclave was heated to 180°C and maintained for 24 h. Next, the precipitate was separated by centrifugation at 10,000 RPM for 5 min. The obtained material was washed several times with distilled water and absolute ethanol to wholly remove redundant components and then dried at 80°C in air for 1 h, successively. Finally, the powder was calcined at 500°C in air for 2 h to obtain pure CeO_2 nanoparticles.

Synthesis of pure CeO_2@Pt

Firstly, 10 mg of the obtained pure CeO_2 powder was dispersed in 30 mL of distilled water and sonicated for 10 min. Then, 0.8 mL of 0.1 M H_2PtCl_6 solution was added and stirred for 10 min at room temperature. Next, 14.4 mL of 0.034 M tri-sodium citrate solution was injected to above suspension. The obtaining solution was heated at 90^{o}C for 4 h, then cooled to room temperature naturally. The color of as-prepared suspension trends to brown. After that, the CeO_2@Pt precipitate was collected by the centrifugation at 18,000 RPM for 30 min to completely separate unnecessary components. Finally, the collected powders were washed with distilled water and absolute ethanol several times, and calcined at 500°C, with the increasing rate of 1°C/min, in air for 2 h to achieve CeO_2@Pt core-shell nanocatalysts.

Preparation of CeO_2@Pt catalytic slurry

10 mg of commercial Pt/C (40 wt.% Pt) composite catalyst was introduced into a 20 mL glass vial. Then, distilled water, 2-propanol and Nafion solution (5 wt.%, Dupont) were added to above vial, respectively. After that, the solution was ultrasonicated at room temperature for 1 h to make sure that the black catalytic slurry was uniformly obtained (Figure S1b).

Preparation of CeO_2@Pt electrocatalyst

Before the spray of Pt/C catalytic slurry, 8 cm^2 carbon cloth substrate was firstly dried at 60^{o}C for 1 h, then was uniformly sprayed an amount of 0.2 mL the CeO_2@Pt catalytic slurry on its surface. Next, the obtained electrode was oven-dried at 60^{o}C for overnight before use.

Preparation of Pt/C catalytic slurry

40 mg of commercial Pt/C (40 wt.% Pt) composite catalyst was introduced into a 20 mL glass vial. Then, distilled water, 2-propanol and Nafion solution (5 wt.%, Dupont) were added to above vial, respectively. After that, the solution was ultrasonicated at room temperature for 1 h to make sure that the black catalytic slurry was uniformly obtained (Figure S1c).

Preparation of Pt/C electrocatalyst

Before the spray of Pt/C catalytic slurry, 8 cm^2 carbon cloth substrate was firstly dried at 60°C for 1 h, then was uniformly sprayed an amount of 0.2 mL the Pt/C catalytic slurry on its surface. Next, the obtained electrode was oven-dried at 60°C for overnight before use.

Table S1 Experimental Conditions for the Working Electrocatalysts Preparation.

Area of carbon cloth (cm^2)	Volume of Pt/C slurry (mL)	Volume of CeO_2@Pt slurry (mL)	Volume of Au@CeO_2@Pt slurry (mL)	Pt loading weight measured by ICP (mg/cm^2)	Electrode denotation
8	0.2	0.0	0.0	0.0543	Pt/C
8	0.0	0.5	0.0	0.0492	CeO_2@Pt/C
8	0.0	0.0	0.5	0.0602	Au@CeO_2@Pt/C

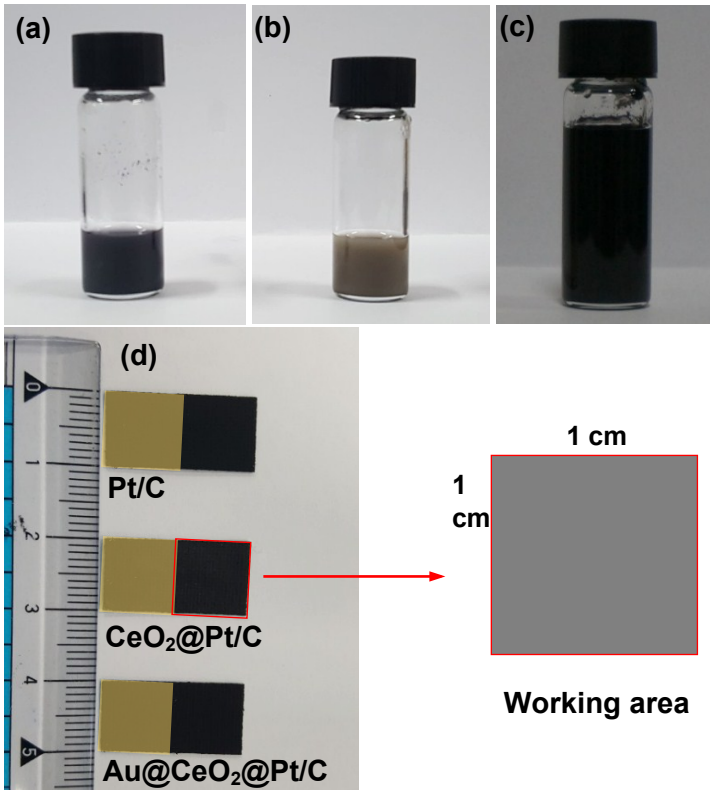

Fig. S1 Photographs of (a) Au@CeO_2@Pt, (b) CeO_2@Pt, and (c) Pt/C slurry, and (d) the corresponding electrocatalysts.

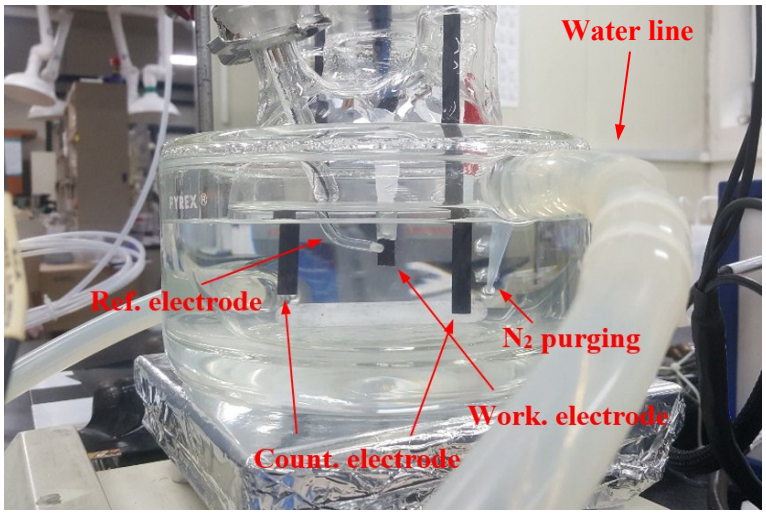

Fig. S2 Setup for the electrochemical properties testing.

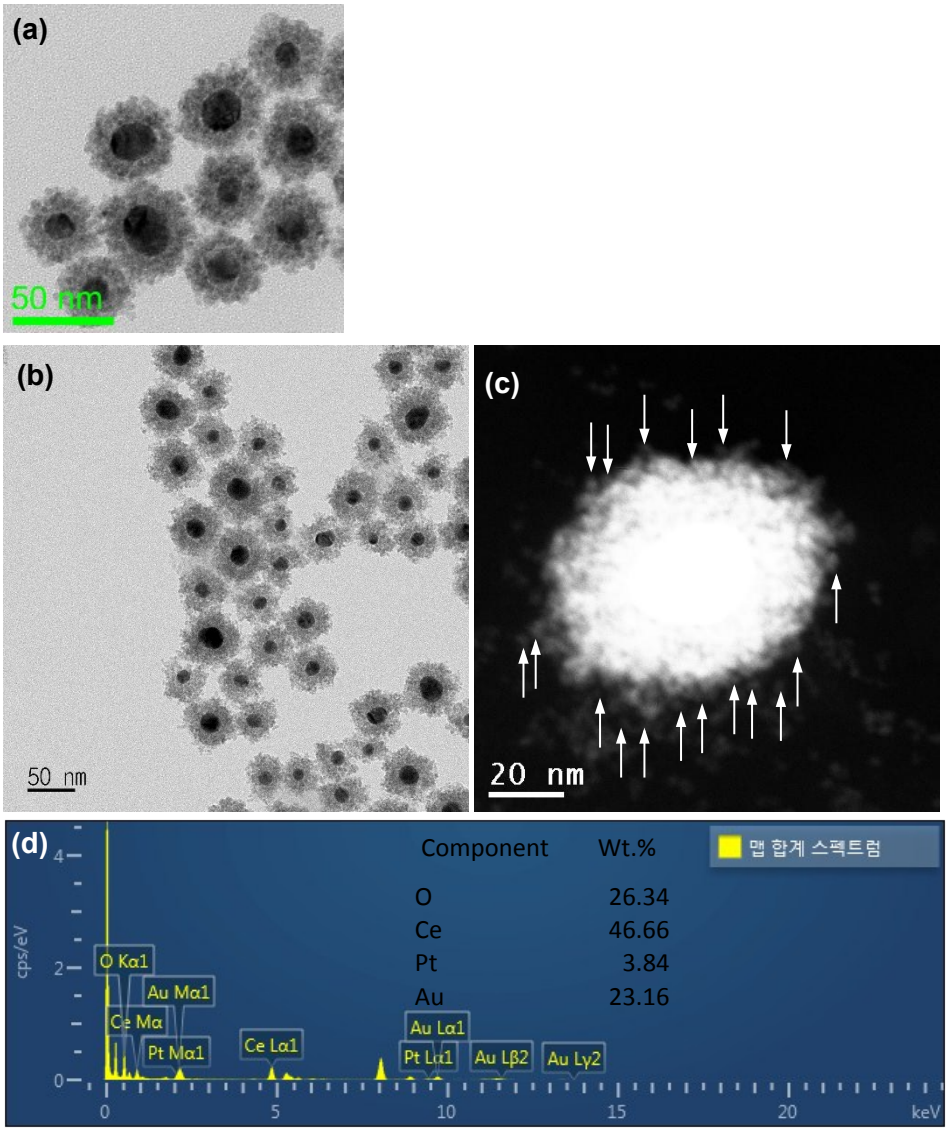

Fig. S3 (a) HRTEM image of single Au@CeO_2, (b) overall HRTEM of Au@CeO_2@Pt, (c) selected particle of Au@CeO_2@Pt with the presence of Pt highlighted by white arrows, (d) EDS spectrum of Au@CeO_2@Pt, showing ultralow Pt loading of 3.84 wt.%.

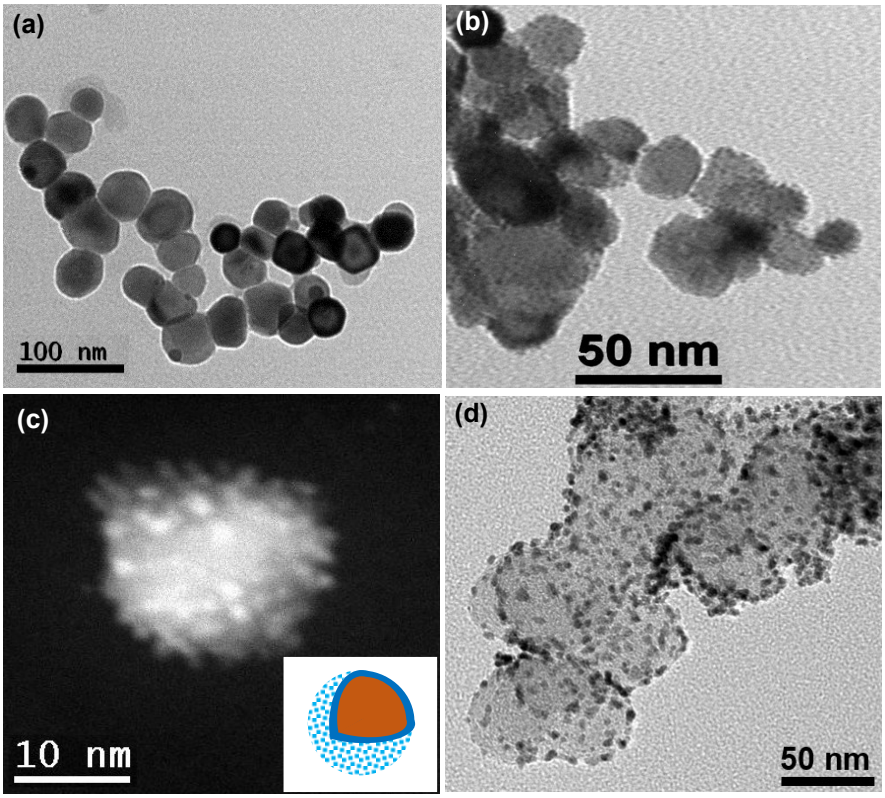

Fig. S4 HRTEM image of CeO_2 (a) before and (b) after coating with Pt, (c) selected single CeO_2@Pt particle, and (d) HRTEM image of Pt/C catalyst.

Fig. S4(a, b) show the HRTEM images of CeO_2 before and after decoration of Pt, in which, the size of CeO_2 supports is around 50 nm. The HRTEM of a single CeO_2@Pt particle is shown in Fig. S4c, with the mean size of about 3 nm. The Pt loading is about 4.08 wt.%. Fig. S4d presents the HRTEM image of the Pt/C catalyst composite; the uniform Pt particles are well dispersed on the carbon black support. The average diameter of Pt catalyst loaded onto the surface of carbon is around 4 nm. The diameter of carbon supports is also found in the range of 40 to 70 nm.

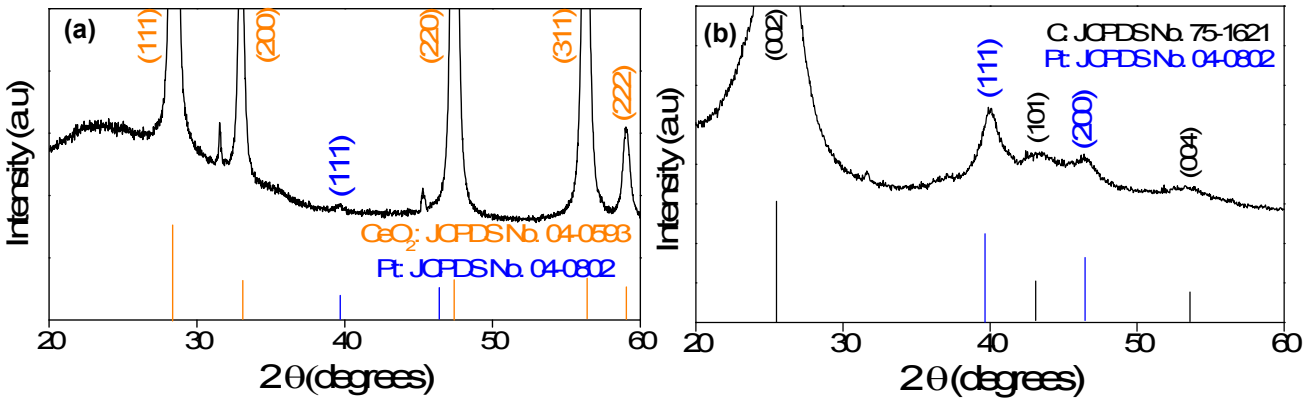

Fig. S5 XRD patterns of (a) CeO_2@Pt and (b) Pt/C catalysts.

Fig. S5(a, b) show XRD pattern of CeO_2@Pt and Pt/C composites, which included Pt peaks marked with blue (well matched to JCPDS No: 04-0802), CeO_2 peaks marked with yellow (well matched to JCPDS No. 04-0593) and C peaks marked with black (well matched to JCPDS No. 75-1621).

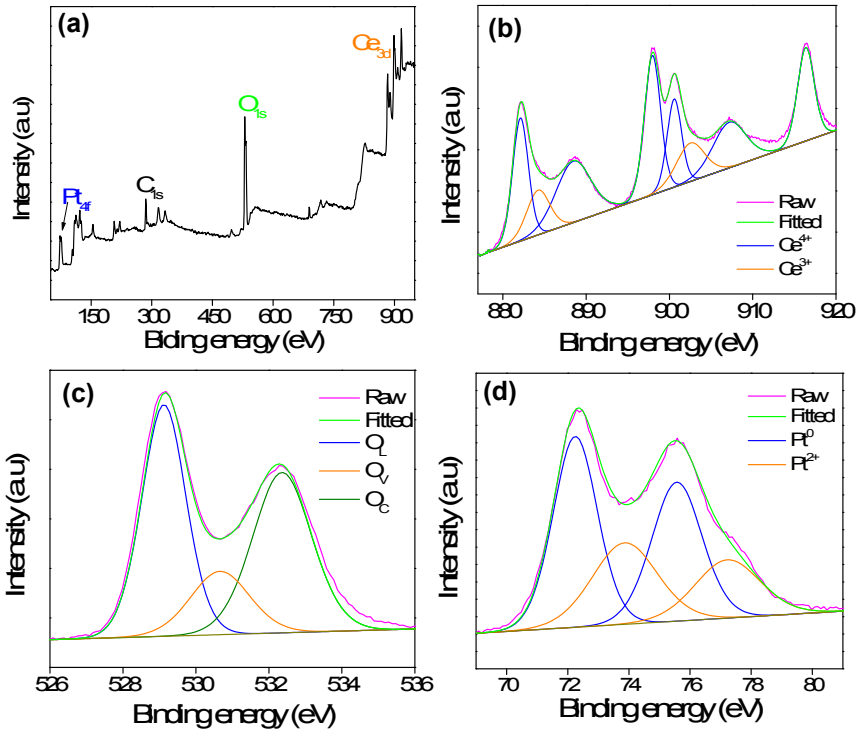

Fig. S6 XPS analysis of CeO_2@Pt catalyst: (a) full spectrum, (b) Ce 3d, (c) O 1s and (d) Pt 4f.

Table S2 Fitting Results of Ce 3d and O 1s XPS for CeO_2@Pt and Au@CeO_2@Pt Catalysts

Catalysts	Ce^{3+}		Oxygen		
	Binding energy (eV)	Relative percentage (%)	Species	Binding energy (eV)	Relative percentage (%)
CeO_2@Pt	884.40 902.80	18.56	O_L (Ce-O)	529.11	47.64
			O_V (vacancy)	530.66	15.24
			O_C (chemisorbed)	532.38	37.12
Au@CeO_2@Pt	884.16 903.04	30.03	O_L (Ce-O)	529.20	54.20
			O_V (vacancy)	530.98	26.46
			O_C (chemisorbed)	532.32	19.34

Table S3 Fitting Results of Pt 4f for CeO_2@Pt and Au@CeO_2@Pt Catalysts

Catalysts	Pt^0		Pt^{2+}	
	Binding energy (eV)	Relative percentage (%)	Binding energy (eV)	Relative percentage (%)
CeO_2@Pt	72.34 75.57	76.86	73.86 77.22	23.14
Au@CeO_2@Pt	72.64 75.96	84.36	74.39 77.69	15.64

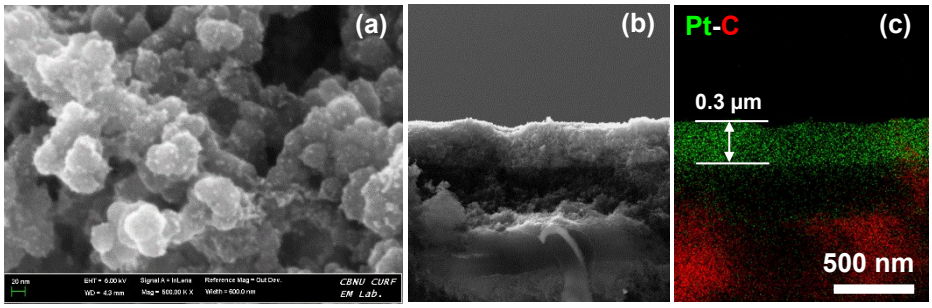

Fig. S7 FESEM surface images of Pt/C: (a) surface, (b) cross-section and (c) EDS mapping.

Fig. S7a shows surface image of Pt/C electrode, in which, the presence of Pt loaded on carbon supports is found as white small dots, and carbon is found as grey particles. The thickness of Pt/C catalyst is observed around 0.3 μm as given in Fig. S7b. Furthermore, the coexistence of Pt (green) and C (red) in catalytic layer is confirmed by EDS mapping in Fig. S7c as well.

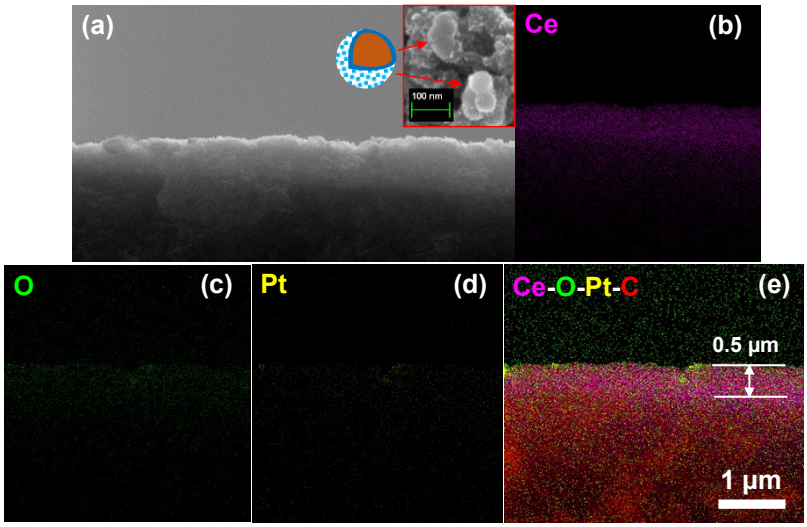

Fig. S8 FESEM analysis of CeO_2@Pt/C: (a) cross-section, the inset showing the surface image, (b-d) EPD mapping and (e) corresponding overlay.

Fig. S8a provides cross-sectional observation of this electrode, with catalytic layer highlighted by white area, the inset shows the surface image of CeO_2@Pt/C electrode, where presence of CeO_2@Pt nanoparticles are illustrated by red arrows with the corresponding model. Mapping of Ce, O and Pt components are revealed by EDS analysis in purple, green, and yellow, respectively (Fig. S8(b-d)). The corresponding overlay is supplied in Fig. S8e, with the thickness of catalytic layer is about 0.5 μm.

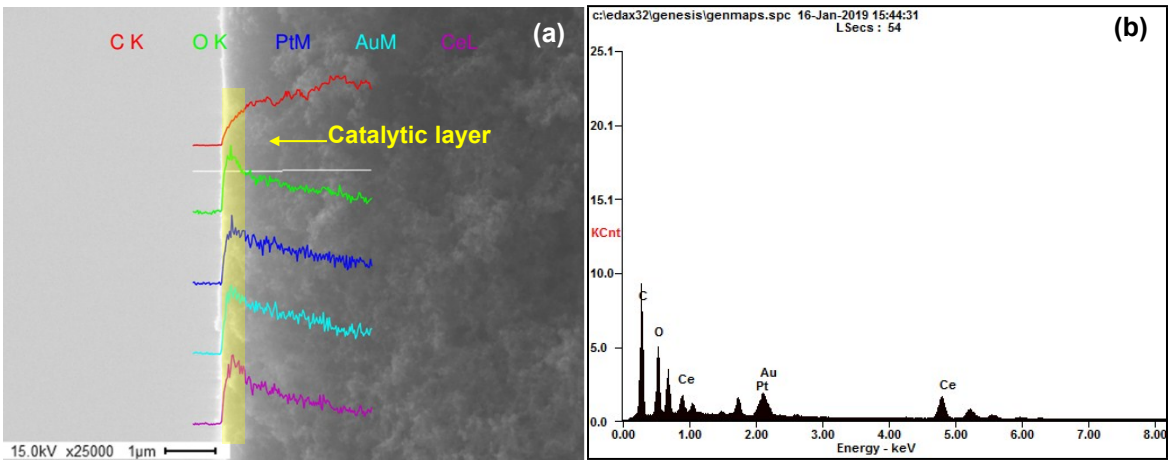

Fig. S9 FESEM-EDS cross-sectional line-scanning and EDS spectrum profiles of Au@CeO_2@Pt/C electrode.

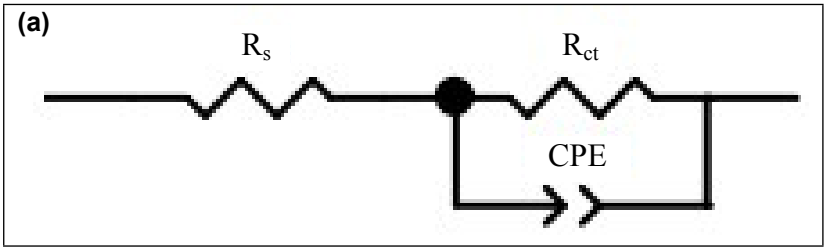

Fig. S10 An electrical equivalent circuit used to fit the Nyquist plots: R_s indicates the solution resistance R_{ct} presents the charge transfer resistance, and CPE is a constant phase element.

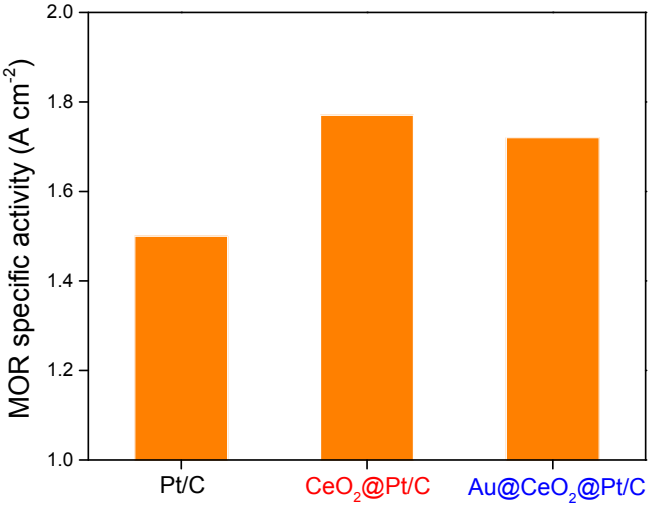

Fig. S11 MOR specific activities of the prepared electrodes. Which were calculated by normalizing the MOR mass activity with the corresponding ECSA.

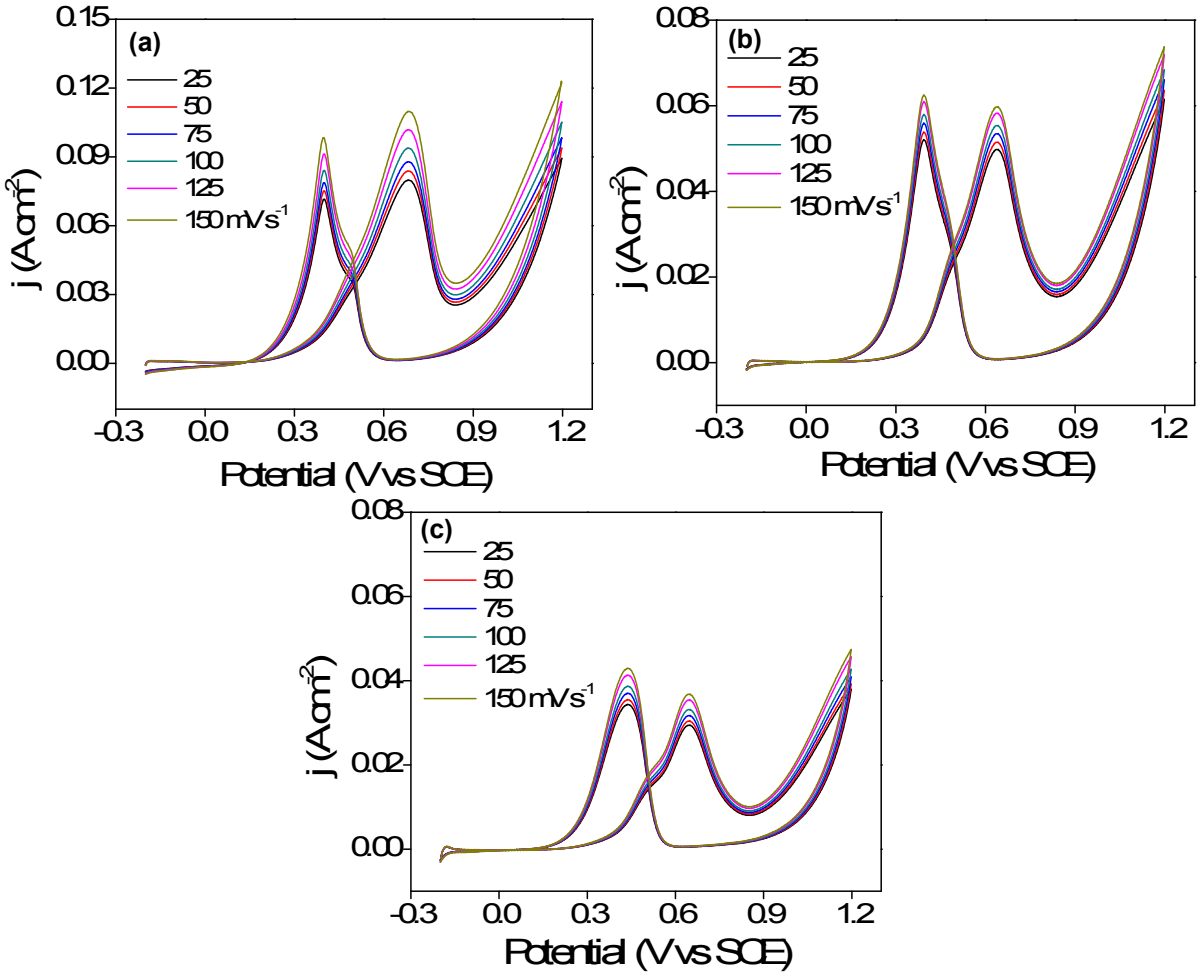

Fig. S12 Sweep rate effect on the MOR performance of (a) Au@CeO_2@Pt/C, (b) CeO_2@Pt/C and (c) Pt/C electrodes in N_2-saturated solution of 0.25 M H_2SO_4 + 1 M CH_3OH at 25°C.

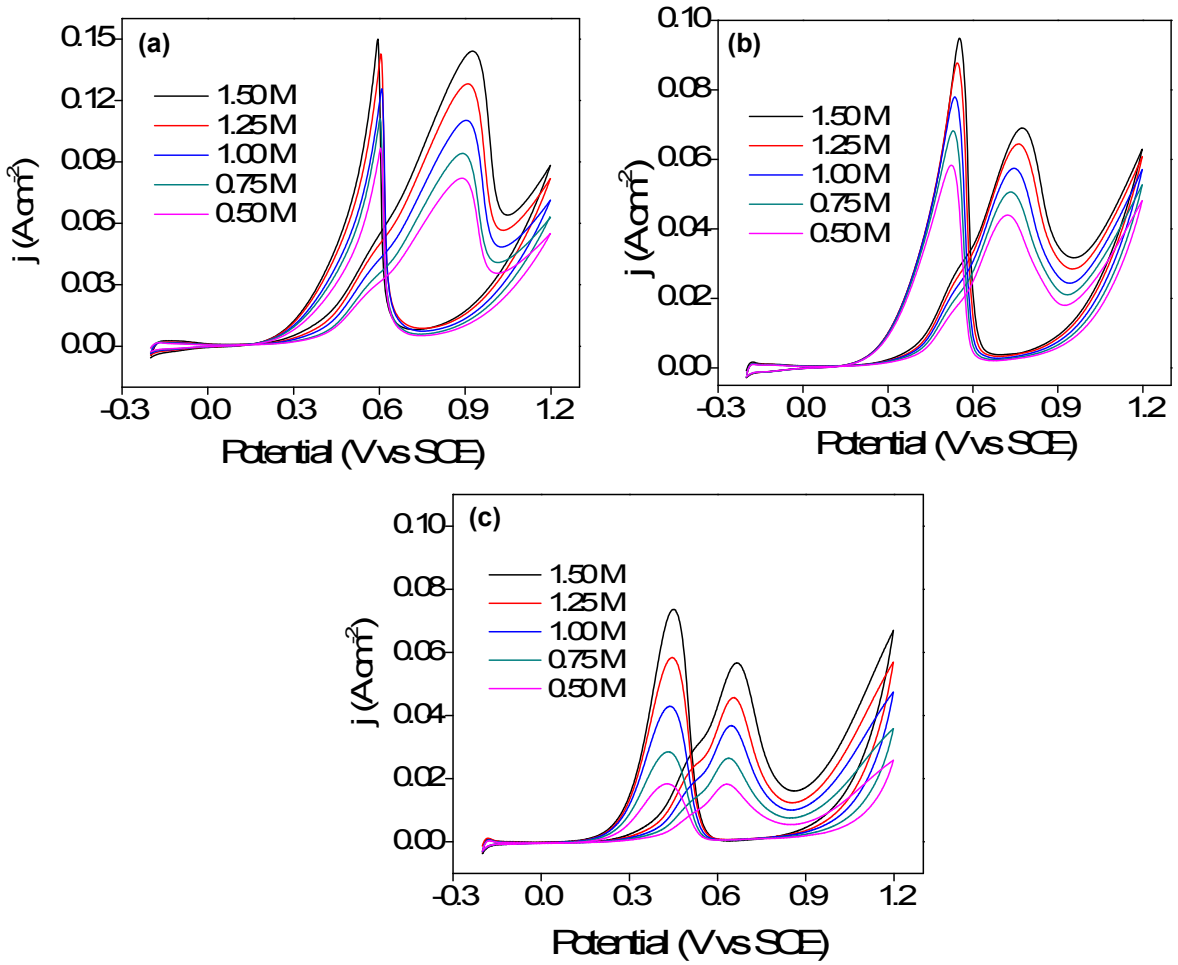

Fig. S13 CH_3OH concentration effect on the MOR performance of (a) Au@CeO_2@Pt/C, (b) CeO_2@Pt/C and (c) Pt/C electrodes at sweep rate of 50 mV s^{-1} at 25°C.

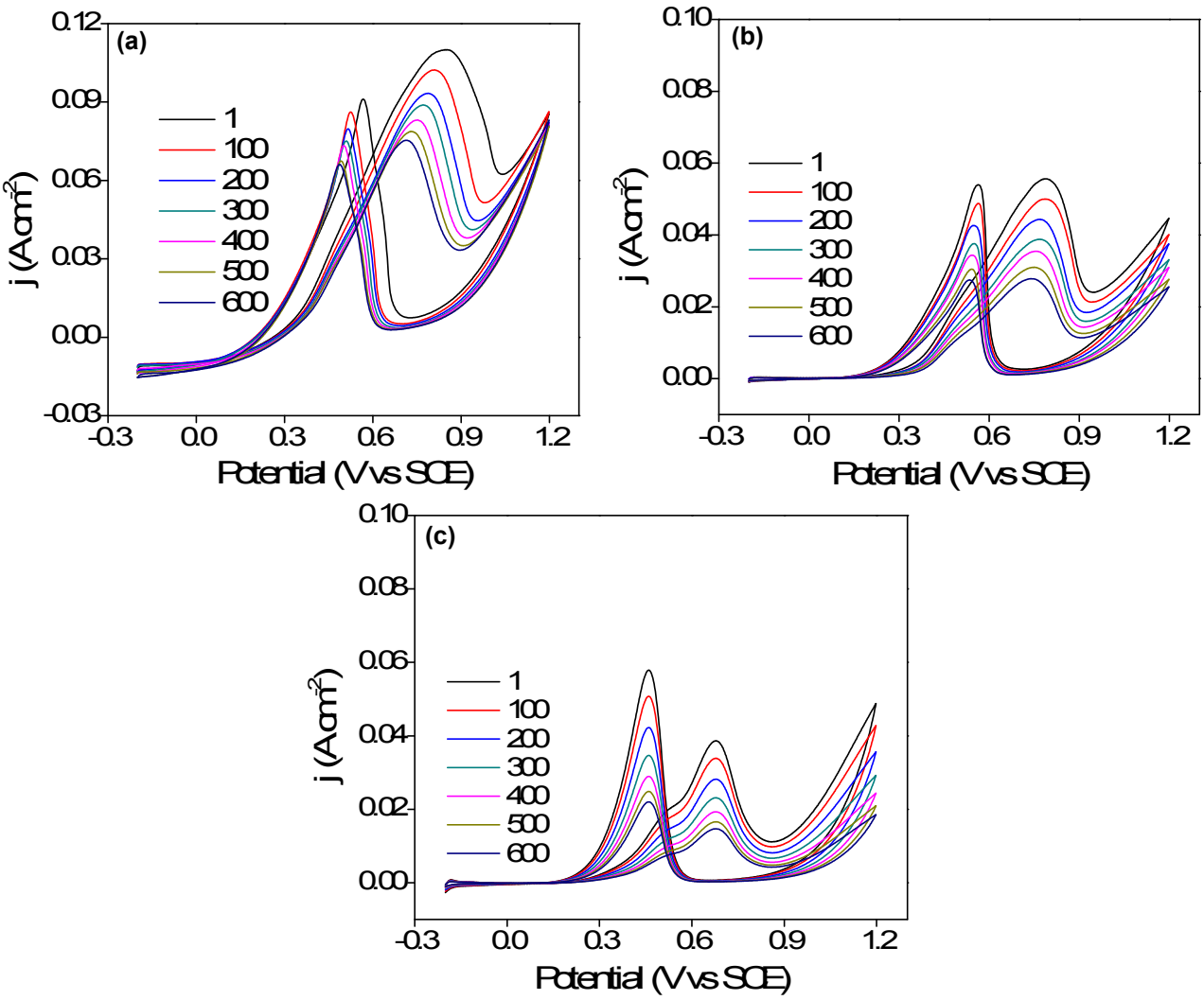

Fig. S14 MOR durability test of (a) Au@CeO_2@Pt/C, (b) CeO_2@Pt/C and (c) Pt/C electrodes in N_2-saturated solution of 0.25 M H_2SO_4 + 1 M CH_3OH at sweep rate of 50 mV s^{-1} at 25°C during 600 sequential cycles.

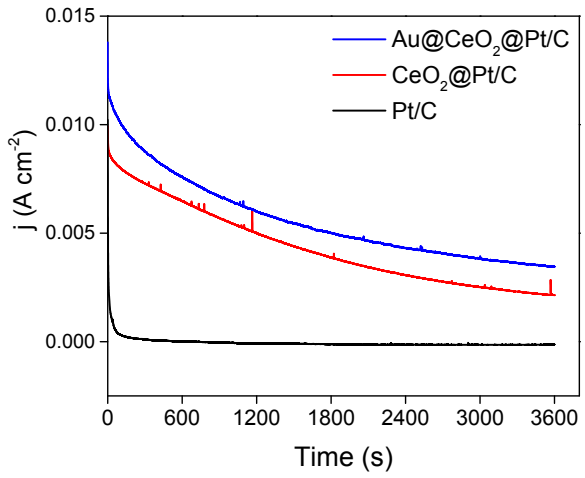

Fig. S15 Chromoamperometric curves of $Au@CeO_2@Pt/C$, $CeO_2@Pt/C$ and Pt/C electrodes recorded in N_2-saturated solution of 0.25 M H_2SO_4 + 1 M CH_3OH at potential of 0.8 V for 3600 s.

Table S4 Comparison of electrocatalytic properties of different Pt-based catalysts for MOR activity

Catalysts	ECSA (m^2/g_{Pt})	Mass activity (mA/mg_{Pt})	Sweep rate (mV/s)	Electrolyte	Ref.
$Au@CeO_2@Pt/C$	**80.0**	**1,360**	**50**	**0.25 M H_2SO_4 and 1 M CH_3OH**	**This work**
Pt/CeO_2/PANI	43.26	360	100	0.5 M H_2SO_4 and 0.5 CH_3OH	1
Shuttle shape Pt/CeO_2	51.00	521	20	0.5 M H_2SO_4 and 1 M CH_3OH	2
Pt_3Pd_1/CeO_2	30.33	853	50	0.1 M $HClO_4$ and 1 M CH_3OH	3
10 % Pt-Ru/CeO_2	134.8	140	20	0.5 M H_2SO_4 and 1 M CH_3OH	4
Pt/CeO_2 (6:4)-RME	N.A.	647	50	0.5 M H_2SO_4 and 1 M CH_3OH	5
Pt/CeO_2/graphene	75.6	366	100	0.5 M H_2SO_4 and 1 M CH_3OH	6
Pt/CeO_2/CNTs	51.5	638	50	1 M $HClO_4$ and 1 M CH_3OH	7
$Pt_{0.89}/SnO_2$/rGO	80.56	519	50	0.5 M H_2SO_4 and 0.5 M CH_3OH	8
$Pt/Ru/SnO_2$ (2.6 nm)	N.A.	440	50	0.5 M H_2SO_4 and 1 M CH_3OH	9
Pt/SnO_2/GNs	92.80	670	100	0.5 M H_2SO_4 and 1 M CH_3OH	10
Pt/WO_3	N.A.	207	50	0.5 M H_2SO_4 and 1 M CH_3OH	11
Pt/WO_3/C-1	76.40	254	20	0.5 M H_2SO_4 and 1 M CH_3OH	12
m-10Pt/WO_3	N.A.	706	50	0.5 M H_2SO_4 and 0.5 M CH_3OH	13
$Pt/HTiO_2$@N-HPCN-	74.80	695	50	0.5 M H_2SO_4 and 1 M CH_3OH	14

800					
PtBi nanoplates	33.9	1,100	N.A.*	0.1 M $HClO_4$ and 0.1 M CH_3OH	15
PtRu NWs	72.1	820	50	0.1 M $HClO_4$ and 0.5 M CH_3OH	16
AgAu@Pt	24.60	483	50	0.2 M KOH and 1 M CH_3OH	17
Pt/NiCo-LDH/NF	131.86	379	50	0.1 M NaOH and 0.5 M CH_3OH	18
Pt/NiFe-LDH/RGO	24.60	949	100	1 M KOH and 1 M CH_3OH	19
PtFe	15.17	537	50	0.5 M H_2SO_4 and 1 M CH_3OH	20
Pt/graphene	51.0	300	50	0.5 M H_2SO_4 and 2 M CH_3OH	21
Pt/[BMIM]BF_4/CNT	N.A.*	155	50	0.5 M H_2SO_4 and 1 M CH_3OH	22
Pt/N-doped graphene	N.A.	400	200	0.5 M H_2SO_4 and 1 M CH_3OH	23
PtAu/N-doped graphene	60.9	417.0	50	0.5 M H_2SO_4 and 0.5 M CH_3OH	24
Pt/B-doped graphene	58.8	410.0	50	0.5 M H_2SO_4 and 0.5 M CH_3OH	25
Pt/N-doped graphene	64.6	390.0	20	1 M H_2SO_4 and 2 M CH_3OH	26
Pt/mesoporous carbon	N.A.	450.0	20	0.5 M H_2SO_4 and 1 M CH_3OH	27
Pt/macroporous carbon	N.A.	81.6	50	0.5 M H_2SO_4 and 0.5 M CH_3OH	28
Pt/N-doped carbon	24.6	343.0	50	0.5 M H_2SO_4 and 1 M CH_3OH	29
Pt/G_3-$(CN)_7$	60.0	612.8	20	1 M H_2SO_4 and 2 M CH_3OH	30

*N.A. was not applicable.

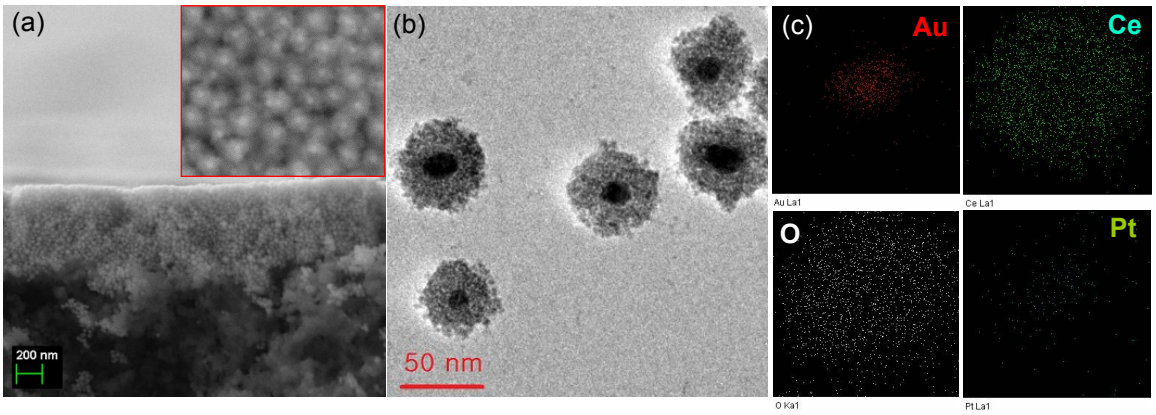

Fig. S16 FESEM and HRTEM analysis confirmation of as-used Au@CeO_2@Pt/C electrode after 600 sequential cycles of the MOR stability test: (a) FESEM cross-section observation, inset giving the surface image, (b) HRTEM image and (c) corresponding HRTEM mapping analysis.

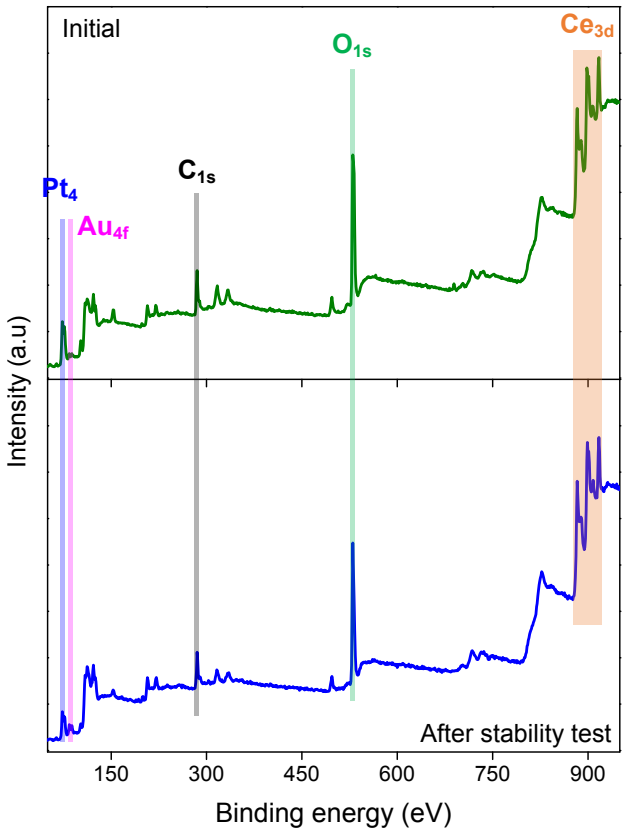

Fig. S17 XPS measurements of Au@CeO_2@Pt catalyst at initial and after MOR stability tests.

The content comparisons of Au@CeO_2@Pt catalyst components (Au 4f, Ce 3d, O 1s and Pt 4f) at initial and after MOR repetitive stability tests (**Fig. S17**) are performed and summarised in **Table S5.**

Table S5 XPS analysis of Au@CeO_2@Pt catalyst before and after 600 sequential cycles of the MOR stability test

Au@CeO_2@Pt	Au^0 (%)	Au^+ (%)	**Ce^{3+} (%)**	Ce^{4+} (%)	O_L (%)	**O_V (%)**	O_C (%)	**Pt^0 (%)**	Pt^{2+} (%)
Initial	87.98	12.02	**30.03**	69.97	54.20	**26.46**	19.34	**84.36**	15.64
After stability	87.67	12.33	**28.76**	71.24	58.52	**23.35**	18.13	**83.51**	16.49

References

1) H. Xu, et al, *ACS Catal*., 2016, **6**, 5198.
2) S.K. Meher, et al, *ACS Catal*., 2012, **2**, 2795.
3) A.B. Yousaf, et al, *J. Phys. Chem. C*, 2017, **121**, 2069.
4) Z. Sun, et al, *Langmuir*, 2010, **26**, 12383.
5) E. Lee, A. Manthiram, *J. Phys. Chem. C*, 2010, **114**, 21833.
6) X. Wang, et al, *Chem. Commun*., 2012, **48**, 2885.
7) J. Wang, et al, *J. Power Sources*, 2007, **164**, 555.
8) S. Wu, et al, *Nano Energy*, 2016, **26**, 699.
9) S. Yang, et al, *J. Mater. Chem*., 2012, **22**, 7104.
10) F. Lei, et al, *Int. J. Hydrogen Energy*, 2016, **41**, 255.
11) J. Mateos-Santiago, et al, *Ind. Eng. Chem. Res*., 2017, **56**, 161.
12) Z. Cui, et al, *J. Power Sources*, 2011, **196**, 2621.
13) X. Cui, et al, *J. Phys. Chem. B*, 2008, **112**, 12024.
14) J. Zhang, et al, *ACS Appl. Energy Mater*., 2018, **1**, 2758.
15) Y. Qin, et al, *ACS Catal*., 2018, **8**, 5581.
16) L. Huang, *J. Am. Chem. Soc*., 2018, **140**, 1142.
17) X. Yan, et al, *Nanoscale*, 2018, **10**, 2231.
18) F. Yang, et al, *Int. J. Hydrogen Energy*, 2018, **43**, 16302.
19) Z. Wang, et al, *J. Electroanal. Chem*., 2018, **818**, 198.
20) X. Zhang, et al, *CrystEngComm*., 2018, **20**, 4277.
21) S.M. Choi, et al, *Carbon*, 2011, **49**, 904.
22) H. Chu, et al, *Adv. Funct. Mater*., 2010, **20**, 3747.
23) B. Xiong, et al, *Carbon*, 2013, **52**, 181.
24) G. Yang, et al, *J. Mater. Chem. A*, 2013, **1**, 1754.
25) Y. Sun, et al, *J. Power Sources*, 2015, **300**, 245.
26) H. Huang, et al, *J. Mater. Chem. A*, 2015, **3**, 19696.
27) H. Jiang, et al, *Chem. Commun*., 2011, **47**, 8590.
28) X. Bo, et al, *Electrochim. Acta*, 2013, **90**, 283.
29) F. Su, et al, *Chem. Mater*., 2010, **22**, 832.
30) H.J. Huang, et al, *Adv. Mater*., 2014, **26**, 5160.